A novel capacitive device for the study of volumetric expansion of hydride powders

Edivagner S. Ribeiro, João M. Gil*

Supplementary Materials

S.1 Equivalent circuit model

In this section we discriminate the components considered in the equivalent circuit model for the sample holder of the capacitive chamber. For its core, which is included within the Gaussian surface defined by the height of the external electrode, we use the geometry of each part of simple symmetry and the electrical properties of the materials to compose the equivalent circuit shown in the diagram of Fig. S.1. We divided this core of the sample holder in three cylindrical sections on top of each other, each corresponding to a parallel line of the equivalent circuit. All components of the chamber outside of the Gaussian surface are included in the complex impedance Z_{out}, determined as described in section S.2.

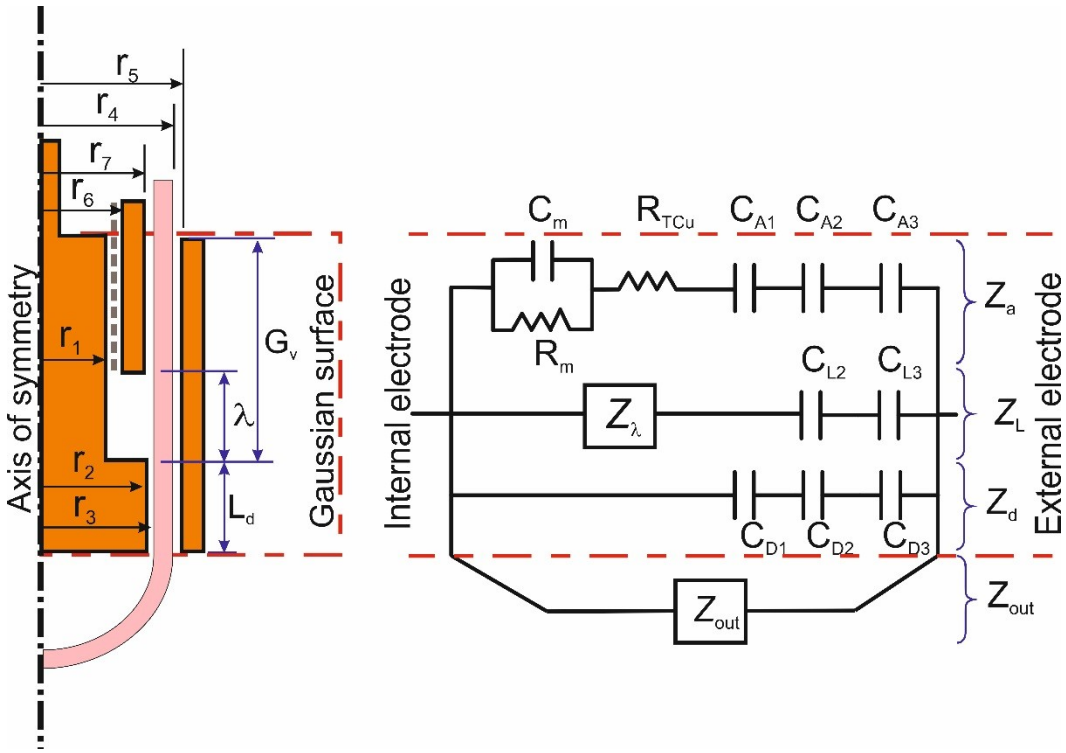

Fig. S.1: Schematic diagram of the capacitive sample holder and its equivalent circuit.

Table S.1 presents the expressions of all components of the circuit of Fig. S.1 that may be defined by their geometry and identifies them with brief descriptions. The schematic diagram in Fig. S.1 defines the relevant dimensions. The overall description of the sample holder is presented in section 3.1 of the main text. In the expressions, ε_{H2} and ε_{Qz} are the electric permittivity of hydrogen and quartz, respectively, and $_{Cu}$ is the resistivity of copper.

Table S.1 – Explicit expressions for the capacitances and resistances considered in the equivalent circuit model

Component	Expression
Copper mesh gas gap capacitance	$C_m = \frac{2\pi\varepsilon_{H_2}(G_v - \lambda)}{\ln(r_6/r_1)}$
Copper mesh resistance	$R_m = \frac{\rho_{Cu}\ln(r_6/r_1)}{2\pi(G_v - \lambda)}$
Copper tube resistance	$R_{TCu} = \frac{\rho_{Cu}\ln(r_7/r_6)}{2\pi(G_v - \lambda)}$
Gas gap between the copper tube and the quartz tube in line “a”	$C_{A1} = \frac{2\pi\varepsilon_{H_2}(G_v - \lambda)}{\ln(r_3/r_7)}$
Quartz tube line “a”	$C_{A2} = \frac{2\pi\varepsilon_{Qz}(G_v - \lambda)}{\ln(r_4/r_3)}$
Gas gap between the external electrode and the quartz tube in line “a”	$C_{A3} = \frac{2\pi\varepsilon_{H_2}(G_v - \lambda)}{\ln(r_5/r_4)}$
Quartz tube in line “L”	$C_{L2} = \frac{2\pi\varepsilon_{Qz}\lambda}{\ln(r_4/r_3)}$
Gas gap between the external electrode and the quartz tube in line “L”	$C_{L3} = \frac{2\pi\varepsilon_{H_2}\lambda}{\ln(r_5/r_4)}$
Gas gap between the internal electrode and the quartz tube in line “d”	$C_{D1} = \frac{2\pi\varepsilon_{H_2}L_d}{\ln(r_3/r_2)}$
Quartz tube in line “d”	$C_{D2} = \frac{2\pi\varepsilon_{Qz}L_d}{\ln(r_4/r_3)}$
Gas gap between the external electrode and the quartz tube in line “d”	$C_{D3} = \frac{2\pi\varepsilon_{H_2}L_d}{\ln(r_5/r_4)}$

Z is a complex impedance modelling the sample space. When a sample is inserted, its equivalent circuit is described in section 3.2 of the main text. Without a sample, Z is the impedance of a simple capacitor with capacitance given by the expression $C_\lambda = 2\pi\varepsilon_{H_2}\lambda/\ln(r_3/r_1)$.

The electric impedance Z_{gauss} of the circuit corresponding to the portion of the sample holder inside the defined Gaussian surface can thus be obtained from the parallel association:

$$\frac{1}{Z_{gauss}} = \frac{1}{Z_a} + \frac{1}{Z_L} + \frac{1}{Z_d} \qquad \text{(S.1)}$$

where Z_a, Z_L and Z_d are the complex impedances of the respective lines of the circuit corresponding to the three portions of the sample holder with heights G_V- , and L_d, respectively.

S.2 Measurement of Z_{out}

In this section, we describe the procedures and the results of the measurements performed to determine the complex impedance Z_{out}, which is an empirical function representing all impedances external to the defined Gaussian surface, to be included in the full equivalent circuit model in parallel with the Gaussian surface circuit (Fig. S.1).

A.C. measurements of capacitance C_{mes} and electric resistance R_{mes} of the chamber as a whole define a complex function Z_{mes} described by the following equation:

$$Z_{mes} = R_{mes} + \frac{1}{i\omega C_{mes}} \qquad \text{S.2}$$

where ω = 2πf is related to the frequency f = 1 kHz used in the electric measurements (section 2.2 of the main text). Results of Z_{mes} acquired without a sample in the chamber are measurements of Z_{cir} with well-defined values of Z_{gauss} (section S.1), with Z as a capacitive reactance derived from a well-defined geometry. The value of Z_{out} can then be obtained from Eq. 3 as follows:

$$\frac{1}{Z_{out}} = \frac{1}{Z_{gauss}} - \frac{1}{Z_{mes}}, \qquad \text{S.3}$$

As referred in section 3.1, Z_{out} depends on the height and on the hydrogen pressure inside the chamber. The sample holder was mounted with the height varying from 3 mm to 6.2 mm. For each value of , readings of pressure, resistance and capacitance were acquired through the Sieverts system and the RLC300 meter as the hydrogen pressure was varied from vacuum to a maximum of 30 bar.

The impedance Z_{out} can be described by its real and imaginary components:

$$Z_{out} = R_{out} + \frac{1}{i\omega C_{out}} \qquad \text{S.4}$$

Fig. S.2 shows the direct experimental measurements of R_{mes} and C_{mes} (Eq. S.2) obtained for the different configurations of the empty chamber.

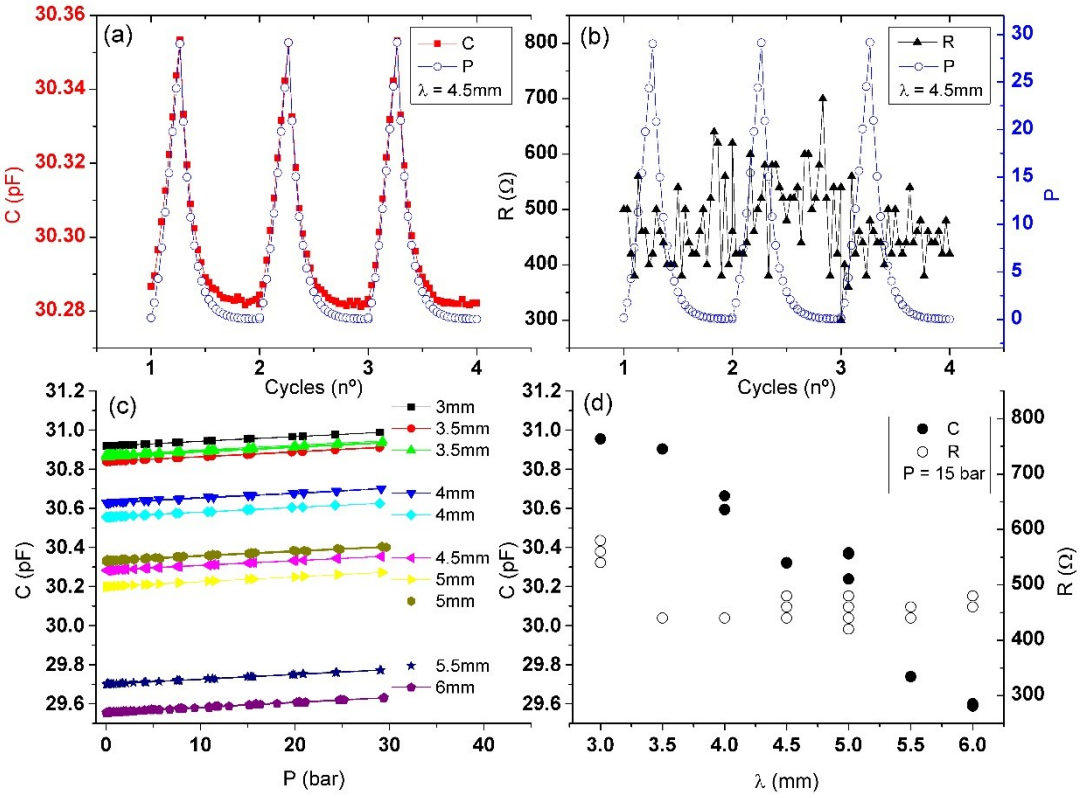

Fig. S.2: Experimental measurements of capacitance and resistance with the empty chamber. (a) Capacitance and pressure along three cycles for = 4.5 mm. (b) Resistance and pressure along the same three cycles for = 4.5 mm. (c) Capacitance for different values of as a function of pressure. (d) Variation of capacitance and resistance as a function of for the pressure of 15 bar.

The measured electric capacitance C_{mes} follows directly the variation of the pressure (example in Fig. S.2a) with a high reproducibility on each pressure cycle. This variation is due only to the linear change of the relative electric permittivity of hydrogen ε_{H2} with pressure [26], similar for all values of (Fig. . S.2c).

The measured electric resistance R_{mes} of the empty chamber shows a constant value, within the measuring uncertainty, as the pressure is varied on each pressure cycle for all values of (example in Fig. S.2b).

Both C_{mes} and R_{mes} present a clear dependency on , as it defines the geometry of the sample holder (Fig. S.2c and Fig. S.2d).

To obtain C_{out} and R_{out} we solve Eq. S.3 for each individual measurement corresponding to a single pair of values (P,). In the calculations, Z_{gauss} takes values derived from the respective geometry of the empty chamber (section S.1).

As expected, the real component does not vary with the pressure but is dependent of . Accordingly, we take only the average value of R_{out} for each pressure cycle and plot them as a function of in Fig. S.3, where an exponential tendency is observed with an asymptote at the higher values of . A least-squares fit of an exponential function to these data, considering three constants (a_r, b_r and c_r),

$$R_{out} = a_r + b_r \exp(-\lambda / c_r) \quad \text{S.5}$$

results in the values presented in Table S.2.

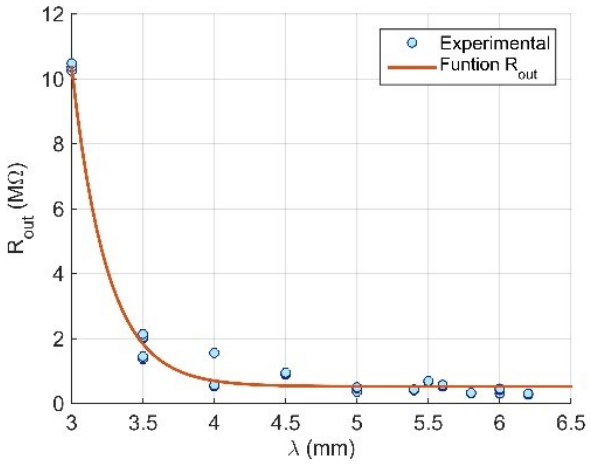

Fig.S.3: R_{out} values calculated from the experimental measurements with the empty chamber as a function of . The red (colour on-line) curve is the result of a least-squares fit of an exponential function to the data.

The values obtained for the capacitive component C_{out} are shown in Fig. S.4. A strong quadratic dependence is observed as a function of , and a linear dependence is observed with the pressure variation (hydrogen permittivity ε_{H2}). In this way, we assume C_{out} to be represented by the following function of and pressure P:

$$C_{out} = (c_0 + \alpha P\lambda + \beta\lambda + \gamma\lambda^2) \times 10^{-12} \quad \text{S.6}$$

The values of the constants presented in Table S.2, were obtained by fitting equation S.6 to the experimental values of C_{out}. The fitted C_{out} function is presented in Fig. S.4 as a surface of variables and P.

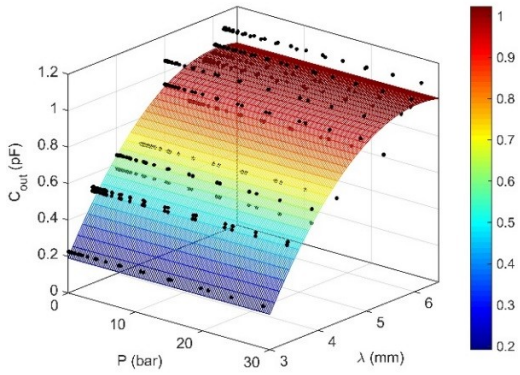

Fig.S.4: Experimental values of the capacitive component C_{out} obtained with the empty chamber and the fitted surface as a function of and P.

Table S.2: Values of the constants defining the components of Z_{out} obtained by fitting Eq.s S.5 and S.6 to the experimental data with the empty chamber.

R_{out}		C_{out}	
a_r	$5.2(5)\times10^{5}$	C_0	-2.211(44)
b_r	$1.7(1.1)\times10^{12}$		1.064(22)
c_r	0.248(13)		-0.0877(25)
			$3.5(2)\times10^{-5}$

S.3 Comparison of the values of each component of the equivalent circuit

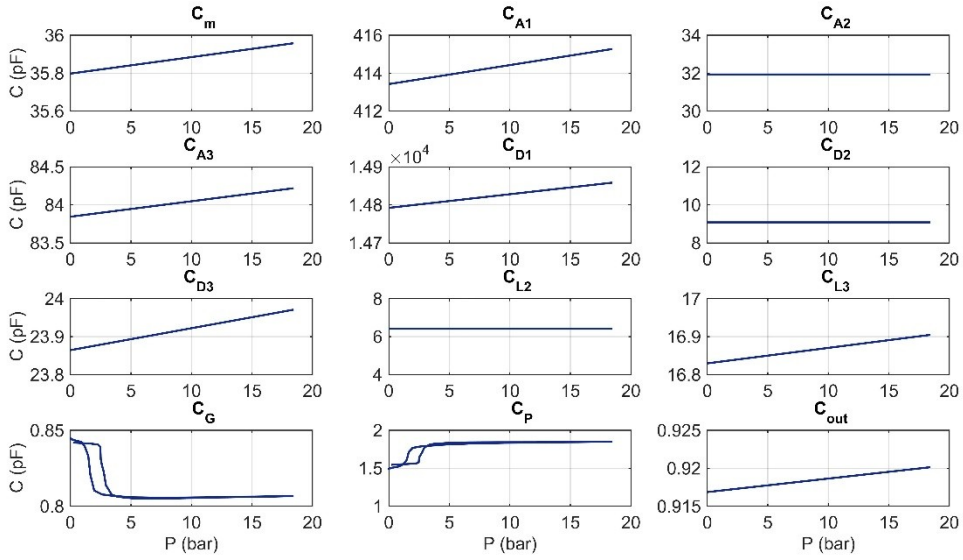

Fig. S.5: Values of the capacitances considered in the equivalent circuit model (Table S.1) for the $LaNi_5$ hydrogen absorption / desorption cycle described in section 4.3 of the main text. All capacitances are shown as functions of the pressure of hydrogen. All values, except the two capacitors of the sample space model (C_G and C_P), are fixed by the geometry of the chamber. Those of gas gaps change with the permittivity of hydrogen.

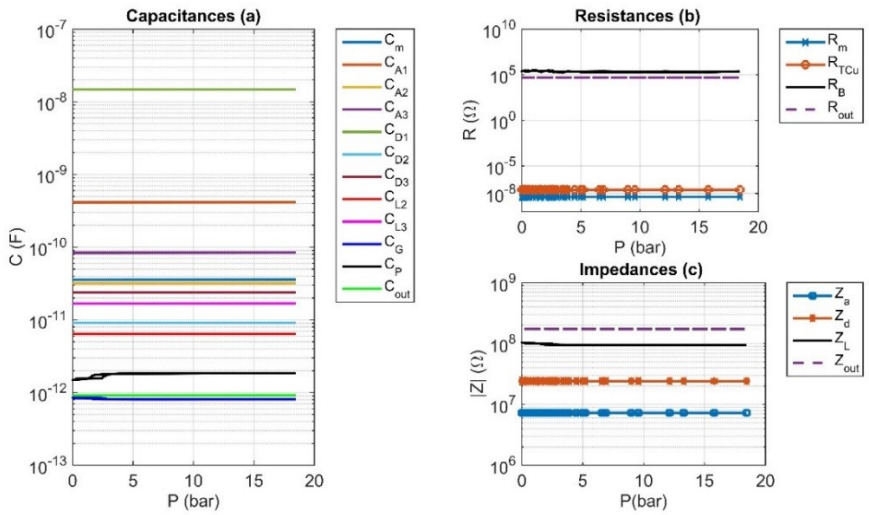

Fig. S.6: Comparison of the values of the capacitances (a), resistances (b) and impedances (c) of the components and lines of the equivalent circuit model for the hydriding cycle described in section 4.3 of the main text. The only changes with pressure visible in the depicted scales are related to the components describing the sample and sample space. All values will change if is changed.

S.4 Calibration procedures and measurements to obtain B_{cn}

As described in section 3.2 of the main text, the empirical function B_{cn} was calibrated through measurements with samples for which we know m, d, L_c and .

Fig. S.7 shows the values of the electric capacitance C_{mes} obtained in the calibration measurements. Clear dependencies on and L_c are observed. The apparent incongruences are related to the dependency on porosity.

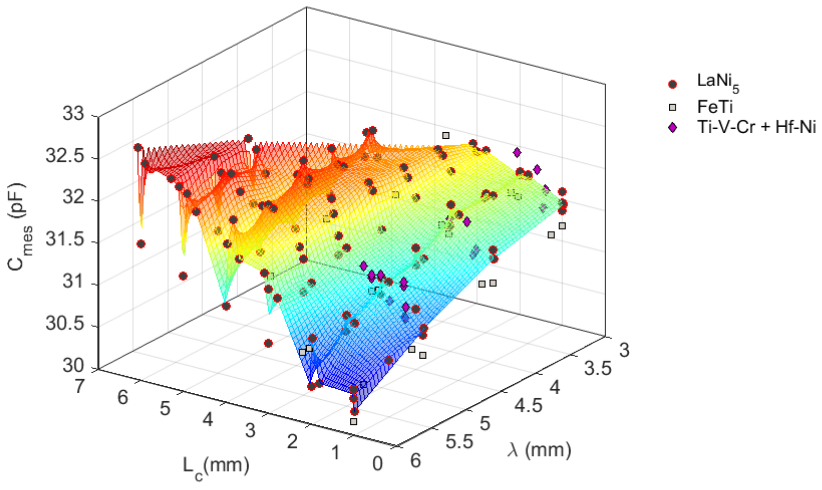

Fig.S.7: Experimental calibration measurements of electric capacitance at atmospheric pressure (air) with variations of porosity (43% - 75%), L_c (1mm – 6mm) and (3mm – 6mm).

The dependency on porosity of both C_{mes} and R_{mes} is presented in Fig. S.8. The dispersion of both parameters for each value of porosity is mainly related to the dependency on and L_c.

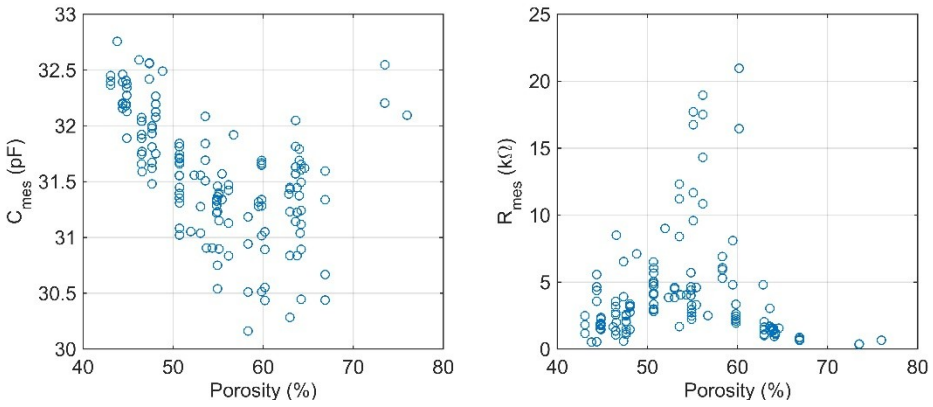

Fig.S.8: Experimental calibration measurements of electric capacitance and resistance as a function of porosity.

All parameters of the global equivalent circuit Z_{cir} (Eqs. 1-6), including the height L_c of the sample, are well defined for each individual calibration measurement except the resistivity and B_{cn}, which are parameters of Z (Eqs. 4 and 6). Therefore, it is possible to obtain the unique pair of values (, B_{cn}) from each corresponding calibration measurement pair (C_{mes}, R_{mes}).

Due to the complexity of the function Z_{cir} (, B_{cn}) of the equivalent circuit model, we used MATLAB to solve the following system of equations for each individual calibration measurement:

$$\begin{cases} R_{cir}(\rho, B_{cn}) = R_{mes} \\ C_{cir}(\rho, B_{cn}) = C_{mes} \end{cases} \qquad \text{S.7}$$

As discussed in section 3.2, B_{cn} depends mainly on porosity (Eq. 7), but as expected, the geometrical parameters of Eq. 6 are not enough to describe the complex geometry of the voids. Here we find that the results obtained for the calibration constant B_{cn} are well represented as a function of and , as depicted in Fig. S.9. The dependency of B_{cn} on L_c is embedded in the dependency on . This distribution of points is well represented by a surface defined by a polynomial of degree 1 in and degree 2 in , expressed by the following empirical equation:

$$B_{cn} = b_{c0} + b_{c1}\lambda + b_{c2}\theta + b_{c3}\lambda\theta + b_{c4}\theta^2 \qquad \text{S.8}$$

Table S.3 presents the values of the 5 parameters of equation S.8 obtained by fitting the polynomial to the experimental calibration points, after centring the scales of the variables on the mean of their experimental values and normalizing to their standard deviation. Fig. S.9 shows the fitted surface superimposed on the calculated values of B_{cn}.

Table S.3: Coefficients of the polynomial B_{cn} (Eq. S.8) fitted to the calibration measurements, with degree 1 in and degree 2 in . is centred on the mean 4.712 and normalized to the standard deviation 1.026, and is centred on 0.5461 and normalized to 0.07816.

	B_{cn}
$\mathbf{b_{c0}}$	5.70(15)
$\mathbf{b_{c1}}$	0.83(11)
$\mathbf{b_{c2}}$	-1.19(11)
$\mathbf{b_{c3}}$	-0.68(12)
$\mathbf{b_{c4}}$	1.02(15)

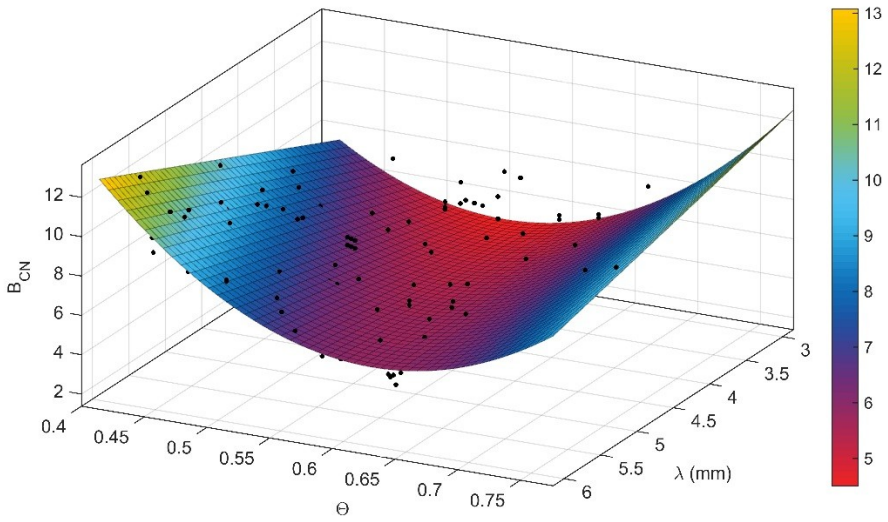

Fig.S.9: Values of B_{cn} obtained from the calibration measurements and fitted surface of the polynomial of Eq. S.8, as a function of porosity and the height .

An eventual dependency of the values of B_{cn} with the permittivity of the gas was investigated with measurements on an unhydrided $LaNi_5$ sample of fixed geometry by varying the pressure, and hence the permittivity, of an inert gas inserted in the sample instead of hydrogen. We chose Ar because it has a higher permittivity than hydrogen, allowing the intended measurements within a reasonable pressure range. Fig. S.10 shows the values of the measured C_{mes} and the values of L_c obtained by using the calibration function and the methodology described in section 4.1 of the main text. In this figure, we converted the values of the pressure and permittivity of Ar to the correspondent values for H_2.

The calculated values of L_c do not vary with the permittivity of the gas within the experimental errors.

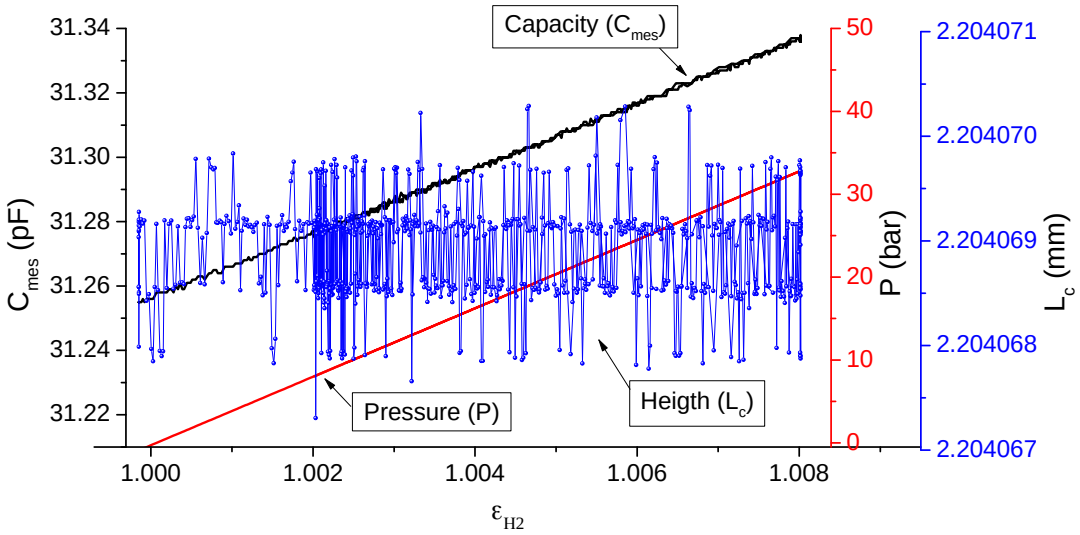

Fig.S.10: Measured capacity C_{mes} and the calculated L_c values obtained on a $LaNi_5$ sample with constant geometry, as functions of the gas permittivity, with varying pressure.

S.5 Hydrogen cycling measurements

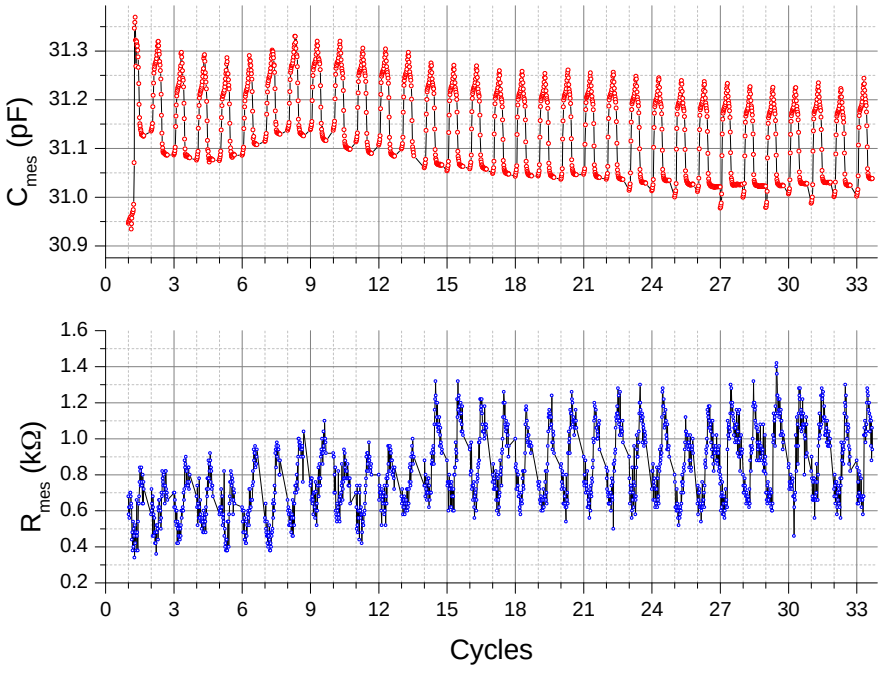

Fig.S.11: Raw data of the electric measurements C_{mes} and R_{mes} on a sample of $LaNi_5$ (0.262 g) as it was cycled through 33 cycles of hydrogen absorption and desorption.